

Novel Recycling to Transform Automotive Waste Glass and Plastics into SiC-Bearing Resource by Silica Reduction

Rifat Farzana · Veena Sahajwalla

Published online: 8 January 2015
© The Minerals, Metals & Materials Society (TMS) 2015

Abstract A significant amount of end-of-life plastics and glass are currently landfilled, incinerated, or just illegally dumped even though conventional plastic and glass recycling practices are well established. This paper describes a novel approach to synthesize silicon carbide (SiC)-bearing product by utilizing waste automotive glass and plastic. The reduction of silica in glass by blend of graphite and plastic (Bakelite) to produce SiC was established experimentally under inert condition at a temperature 1,550 °C. The results from X-ray diffraction, scanning electron microscopy, energy dispersive X-ray spectroscopy EDS confirm the formation of SiC, and the reaction kinetics and the mechanism of reduction were investigated by means of infrared gas analyzer. Rate constant, $k = 12.8 \times 10^{-4} \text{ s}^{-1}$, for the initial stage was measured for overall silica reduction, and the mechanism was established to be predominantly controlled by chemical reactions. This process innovation has two significant advantages: it is a major step toward transforming nonmetallic automotive waste into valuable resources like SiC-containing refractory materials, and it reduces the industry's reliance on conventional raw materials including quartz and coke which are typically used as silicon and carbon bearing resources.

Keywords Automotive waste glass · Waste plastics · Silicon carbide · Refractories

Introduction

Carbothermic reduction of silica in submerged electric arc furnace is a conventional route for producing SiC [1]. Commercial SiC is produced by the Acheson process from direct reduction of silica with petroleum coke. The reduction is a strong endothermic reaction, which requires temperatures in the range of 2,000 and 2,500 °C, and hence the process uses 6.5–11 kWh of electrical energy for the production of 1 kg of SiC [2]. However, the source of conventional carbonaceous materials like coke/coals are becoming scarce, and recycling of byproducts and wastes will be an emerging critical issue in near future [3]. Therefore, recycling waste automotive glass as silica source along with blend of plastic and conventional carbon as reducing agents could provide an innovative way to synthesize SiC.

SiC refractories are found as both non-oxide and composite refractories, and may contain components such as silicon carbide, graphite, silicon, silica, silicon nitride, periclase, mullite, andalusite, cristobalite, corundum, and other phases that contain iron, calcium, titanium, etc. as impurities [4]. SiC and carbon (graphite), as refractory materials, are used in some very severe temperature conditions due to high thermal conductivity together with high thermal strength and low thermal expansion, and resistance to chemical reaction [5].

About 750,000 cars reach the end of their lives (ELV), each year in Australia alone [6], and the generation of ELVs was estimated to be 40 million worldwide in 2010 [7]. A domestic vehicle weighs roughly one tonne of which around 16 % is made of glass and plastics [8]. Thirteen different plastics are used in cars [8] and two types of flat/float glasses: laminated glass and tempered glass are commonly used as windshield and window glass in modern vehicles.

R. Farzana (✉) · V. Sahajwalla
Centre for Sustainable Materials Research and Technology
(SMaRT)@UNSW, School of Materials Science and
Engineering, UNSW Australia, Sydney, NSW 2052, Australia
e-mail: r.farzana@student.unsw.edu.au

While offering many benefits in safety, usability, and durability, the technological evolutions in manufacturing of these components are also increasing the complexity of recycling. In windshield and architectural glass, polyvinyl butyral (PVB) sheets are interleaved to form float glass laminate. The PVB plastic laminate interlayer in such glasses makes it much more difficult and expensive to recycle as the glass has to be first separated from the interlayer using mechanical techniques [6]. Furthermore, the PVB itself cannot be recycled due to the glass scrap that remains attached [9]. Tempered glass is produced at high temperature followed by quenching. Tempered glass is not mixed with conventional container glass recycling due to their different melting temperatures [10]. The plastic waste in ELV is a complex mixture due to the blending of different plastics during the manufacturing process, and contamination throughout the vehicle's lifetime. Therefore, recycling of ELV glass and plastic is difficult and expensive because of additional processing, sorting, and cleaning, and thus destined to landfill.

Studies have been carried out in our group to investigate the use of plastics as carbon sources in steelmaking [11, 12]. Recently, we reported the use of waste CD as carbon source to produce SiC nanoparticles. Using silica and conventional carbon sources, many studies [13–17] were carried out to investigate carbothermic reduction kinetics, effect of contact areas, and their mechanisms. However, with regard to replacing conventional carbonaceous material with waste to produce SiC, only a few studies [18, 19] were reported in the literature.

In this study, a novel solution has created a new resource from automotive waste glass and plastics together, through their chemical transformation into SiC. Synthesis of SiC-bearing product from waste auto glass as silica source and blend of plastics (Bakelite) and graphite as reducing agent in presence of iron is reported. In our approach, the integral plastic layer in glass is not a problem and instead could become a carbon resource. Investigation on silica reduction reaction kinetics and associated mechanisms to transform waste into a resource containing SiC is also conducted. Synthesized SiC along with other unreduced oxides (such as SiO₂, CaO) from waste glass and carbon from graphite could in turn serve as raw materials in manufacturing SiC-bearing refractories in the future.

Experimental

Silica is the dominant oxide (approximately 70 %) of automotive glass along with several oxides. The composition of the waste windshield and window glass collected from Campsie Automotive Glass Pty Ltd, Australia is given in Table 1. Thermoset plastic, Bakelite, was

characterized by XRD showed mainly calcium carbonate with a small amount of silica impurity (Fig. 1). Chemical analysis of Bakelite is also given in Table 2 and 3. Graphite (~99 %) and iron oxide (Fe₂O₃) powder ≥99 %, was also used for this study.

Waste automotive glass and Bakelite were ground to powder using a ring mill for 2–3 min. Waste automotive glass and carbonaceous material (blend of 33 wt% graphite and 67 wt% Bakelite) were used in an approximate stoichiometric ratio to produce SiC (reaction 9). The use of iron oxide made a significant change in the reduction mechanism and SiC formation due to substantial amount of CO generation [20]. Thus, a small amount of iron oxide (11 wt%) was also added in the mixture. All reactant materials were transferred in a glass jar, and the jar was kept on the roller milling machine which was rotating at approximately 2,000 rpm, for more than an hour to ensure the homogeneity of the reactant mixture. Then, by adding water, spherical-shaped pellets were made by hand in order to minimize the contact of the sample with the crucible. Pellets were dried in the oven for more than 12 h at 90 °C to remove any moisture content.

The schematic diagram of the experimental set up is shown in Fig. 2. The horizontal tube furnace was fabricated from double-walled, vacuum-insulated stainless steel frame fitted with a fan cooler to dissipate heat. The furnace tube was 1 m long and of 50 mm inner-diameter, and the hot zone where the temperature was 1,550 °C, it was 150 mm long. The tube is made of alumina, and the rod holding the crucible is made of carbon. Crucibles composed of zirconia (51 wt%), silica (39 wt%) and alumina (3.7 wt%) were used for this study, and the pellet was placed on the crucible. Constant argon (high purity, 99.99 %) flow rate 1 L/min was maintained throughout the

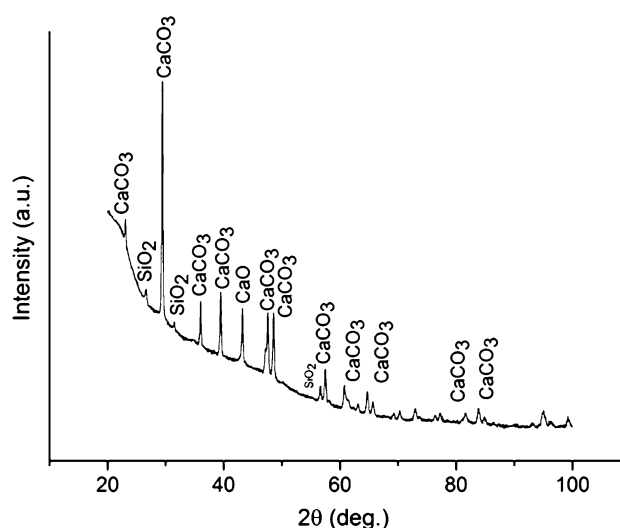


Fig. 1 X-ray diffraction pattern of raw bakelite

Table 1 Major oxides in windshield and window glass (analysis done by XRF) (oxides <0.2 wt% are ignored)

Compound	Windshield (wt%)	Window (wt%)
SiO ₂	71.001	69.211
Na ₂ O	14.537	15.016
CaO	8.519	9.159
MgO	3.918	3.608
Fe ₂ O ₃	0.559	0.587
Al ₂ O ₃	0.510	1.234
K ₂ O	0.172	0.441
Total	99.216	99.256

Table 2 Chemical composition of Bakelite

Composition (wt%)			
Ultimate analysis		Proximate analysis	
Total carbon	53.4	Fixed carbon	31.70
Hydrogen	4.0	Volatiles	47.55
Oxygen	11.6	Moisture	3.01
Sulfur	0.017	Ash	17.74

Table 3 Composition of ash of Bakelite (analysis done by XRF)

Compound	CaO	SiO ₂	SO ₃
wt%	94.53	5.14	0.33

experiment using a mass flow meter. The sample was pushed slowly into the hot zone to begin the reduction reactions when the required temperature (1,550 °C) was achieved. At the end of the desired reaction time, sample was pulled to cool down, and then analyzed. IR gas analyzer unit (Advance Optima model ABB® AO2020) was attached to the furnace to measure the gases evolved from

the reduction reactions, and off gases showed approximately 30 s time lag to reach the sensor of the IR. The reaction products were characterized by XRD (Philips Multipurpose X-ray Diffraction system) and SEM (Hitachi 3400-I), and topographic elemental investigation was made by EDS (Bruker X flash 5010). The in situ reduction of pellet was captured using a video camera (SANYO, high resolution CCD) connected to the DVD player, displaying reaction visually at high temperatures.

Results and Discussion

A sequence of video images recorded over 15-min time period at 1,550 °C in the hot zone of the furnace for observing in situ reduction is shown in Fig. 3. Over time, the pellet started showing visible signs of reduction, evident from escaping gases (CO, CO₂, and CH₄ off gases in the Infrared gas analyzer). The pellet showed sharp reduction in volume over time and demonstrated the occurrence of rapid reduction reactions and some extent of melting. After 8 min, as the pellet size became smaller than the crucible depth, it was not possible to capture those images. The last image in Fig. 3f shows the reduced pellet photograph taken outside the furnace at room temperature.

The XRD pattern of the reduced pellet is shown in Fig. 4. Strong and sharp diffraction peaks of cubic β-SiC were observed along with carbon and low-intensity silica peak, and Fe₅Si₃. The hump observed initially is due to amorphous phases particularly from oxides that form a thin glassy layer on top. XRD semiquantitative analysis using X’pert Highscore Plus software showed more than 50 % SiC formation in the reduced sample within 15 min. Rather than Si, C, and Fe, the EDS analysis (Fig. 5) identified Ca, K, Al, Na, O, etc. in the reduced product. These elements were assumed to be from low concentration oxide formed

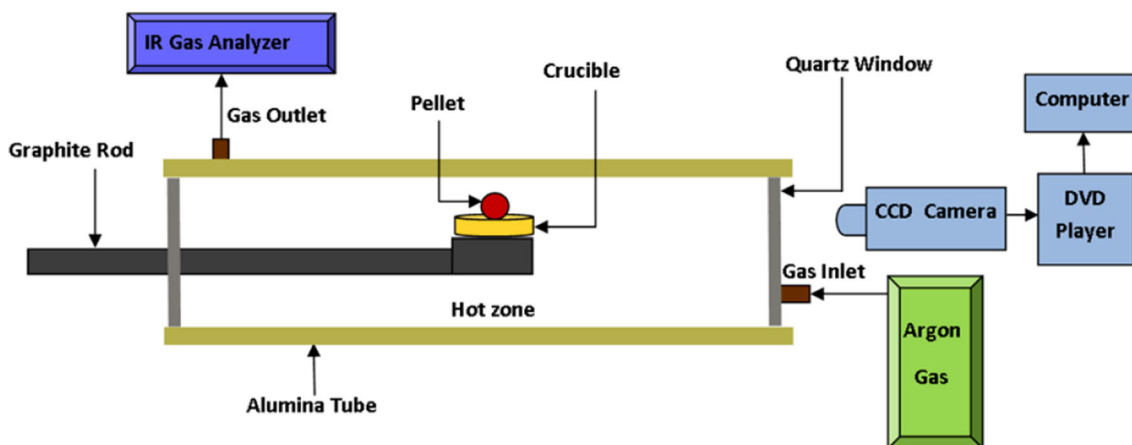


Fig. 2 Horizontal tube furnace arrangement

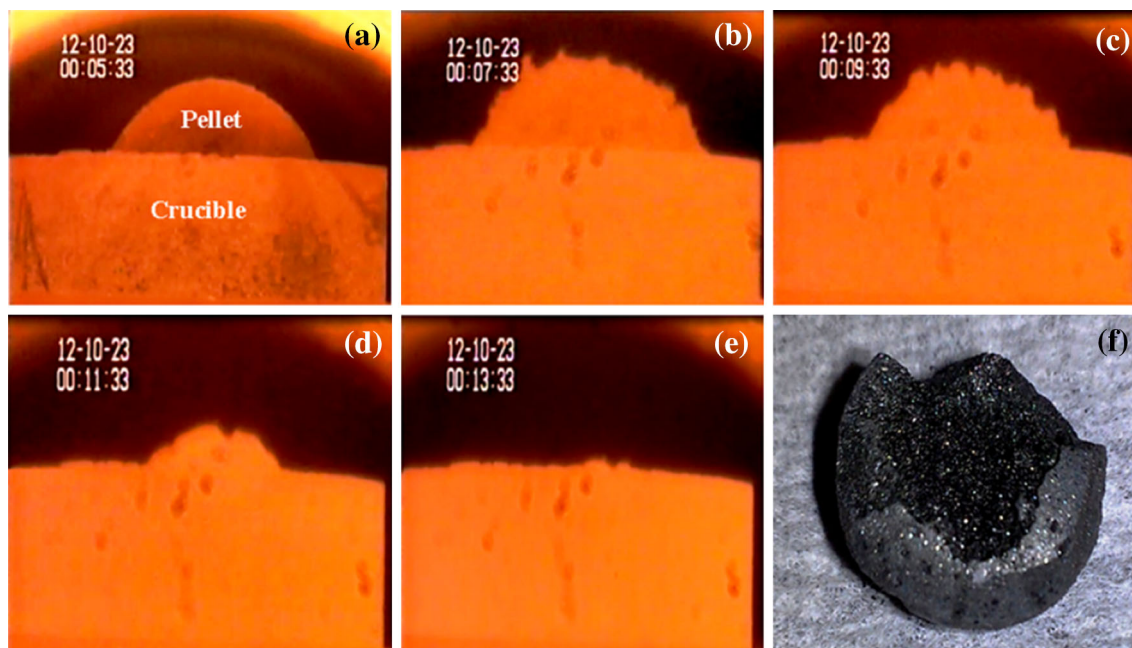


Fig. 3 In situ reduction of pellet in hot zone at temperature of 1,550 °C. **a** 0 min, **b** 2 min, **c** 4 min, **d** 6 min, **e** 8 min, **f** reduced pellet after 15 min at room temperature

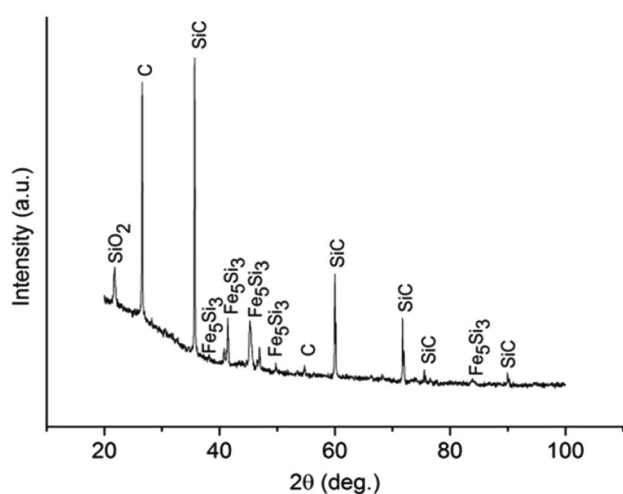


Fig. 4 XRD spectrum of reduced pellet after the reduction time of 15 min

or fayalite or other silicates, as XRD did not show any crystalline phases except SiC, Fe_5Si_3 , SiO_2 , and C. Cr peak was from the chromium coating to make the sample conductive. However, acid leaching of the final product can be conducted to reduce the concentration of oxide/silicates impurities, as most of the metal oxides are soluble in acids like HCl, HNO_3 , etc., and silicates are soluble in HF or $\text{HF} + \text{H}_2\text{SO}_4$. Phase analysis using point scan method by EDS was done at higher magnification of $500\times$ (Fig. 6) on reduced pellet after 4-min time period in hot zone. Points were selected at different phase areas. Points 2, 3, and 7

visually looked to be in the same phase and were bright in color, which represents iron-rich areas. Iron, silicon, and carbon were detected in the EDS spectra. So it could be attributed to the formation of Fe_5Si_3 . Points 5, 6, and 9 showed a high amount of carbon and small amounts of oxygen and iron. This explains why this area appears darker in the image. Within the reaction time 4 min, although some amounts of the silica and iron oxide were reduced by carbon, this area was rich in carbon due to the availability of excess carbon for the rest of reduction reactions. The presence of iron and oxygen could be due to partial reduction of Fe_2O_3 to FeO or unreduced hematite or silica. The gray intermediate areas are represented at points 1, 4, and 8. These points showed high-intensity silicon peak compared to other points. Beside silicon, other metals including iron, calcium, sodium, magnesium, aluminum, and potassium peaks were also visible. Carbon and oxygen peaks were also present in the spectra. These areas could be attributed to some nucleation of SiC and the presence of other impurities such as sodium, calcium, magnesium potassium, and/or some other complex compounds along with silica or FeO– SiO_2 melt. Calcium peak was notably high and could be attributed to Bakelite degradation.

Thermoset plastic Bakelite structure starts to dissociate at 350 °C, and weight losses at 600–800 °C are attributed to degradation of both Bakelite and calcium carbonate [21]. In order to understand Bakelite's behavior at high temperatures, some trial runs were carried out with only Bakelite powder following the same experimental

Fig. 5 Overall EDS spectrum of reduced pellet after the reduction time of 15 min

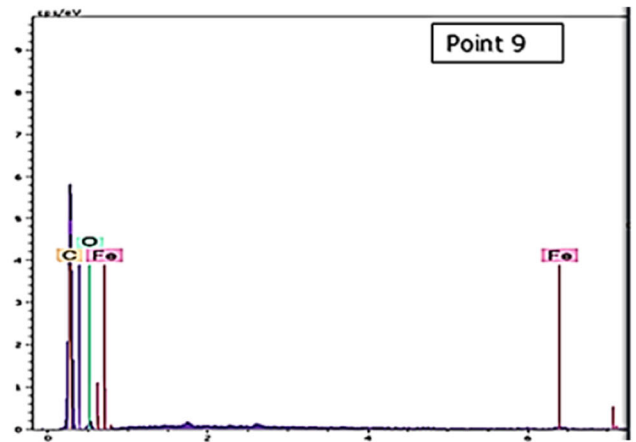
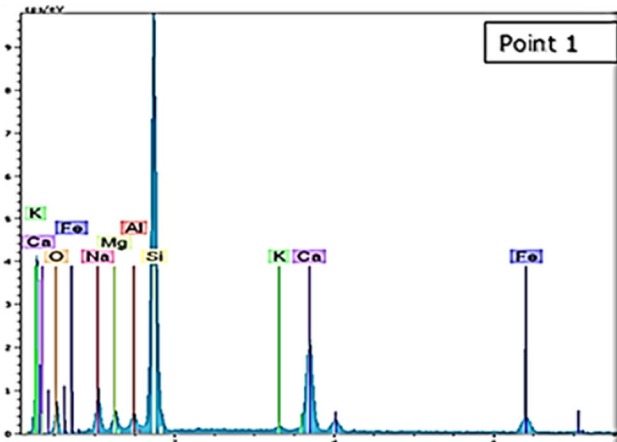
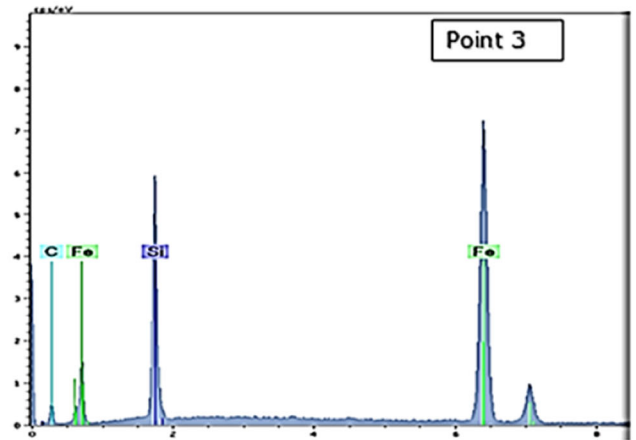
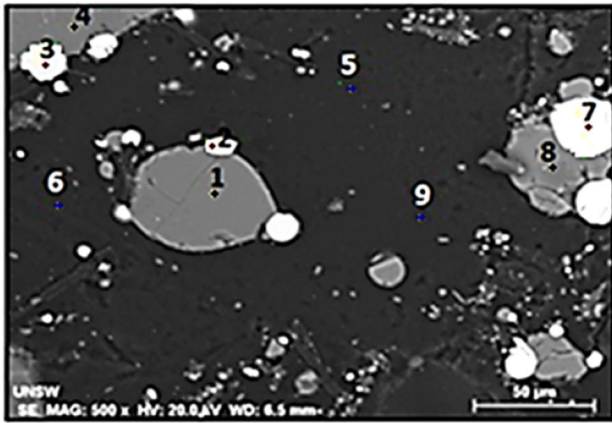
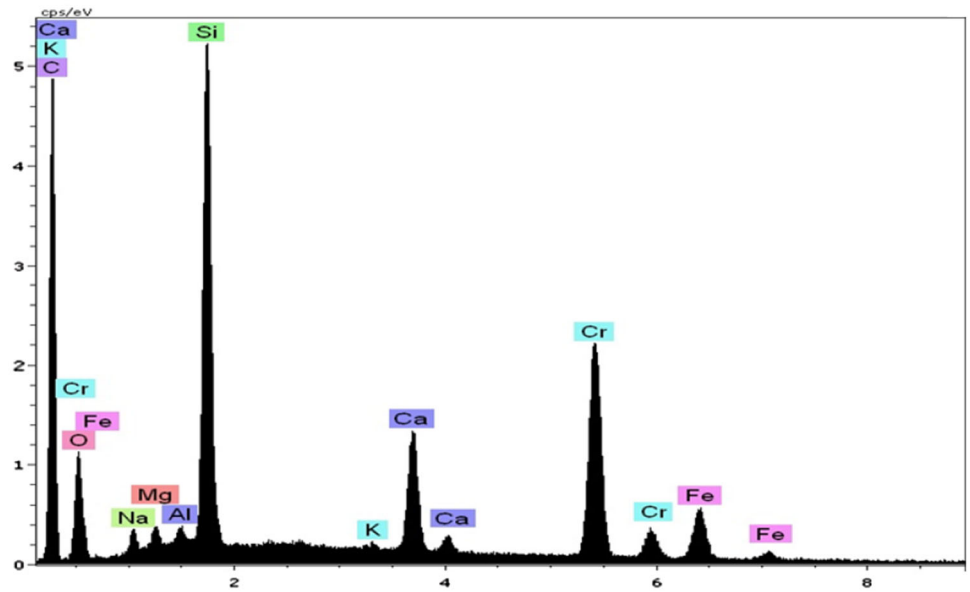


Fig. 6 Point scans profile by EDS of reduced pellet after the reduction time of 4 min

procedure. Nearly 60 % weight loss occurred at 1,550 °C within 15 min, and this could be attributed to volatile release and removal of gases such as CO, CO₂, and CH₄.

Residual 40 % char was characterized by XRD and LECO carbon analysis. In XRD pattern, Ca₂SiO₄, C, CaC₂, and SiC phases were found (Fig. 7), and carbon analysis

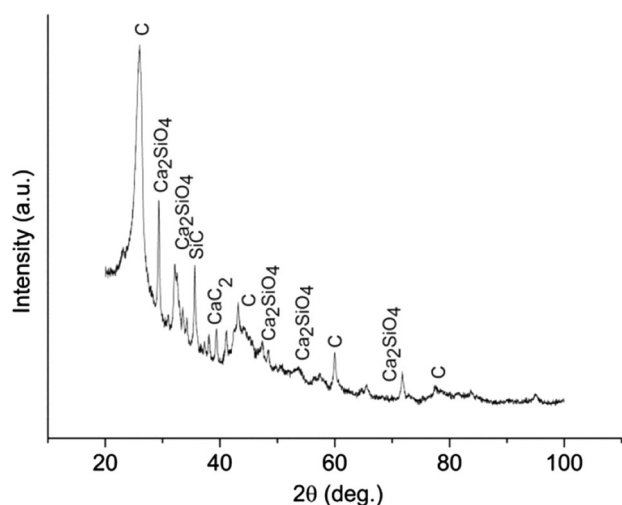


Fig. 7 XRD of Bakelite char at temperature 1,550 °C at the reduction time of 15 min

showed carbon content of 73.16 wt% in residual char. The rate of formation of SiO (reaction 5, 6) is enhanced by CO/CH₄ for silica/silicate slags [20, 22], and iron oxide reduction by CH₄ is also established [11]. Therefore, CO and CH₄ from Bakelite as reducing gas and produced char as a solid carbon source along with graphite blend should enhance the reduction reactions.

Samples were analyzed by varying reduction times (2, 4, 6, 8, and 15 min) by XRD technique (Fig. 8) along with SEM images to understand the formation of different phases over time. From the hot zone, samples were taken out at different reduction times to room temperature for analysis. Up to 8 min in the hot zone, hexagonal quartz was observed in XRD rather than the tetragonal cristobalite peaks. Thermodynamically, iron oxide reduction is much easier than silica reduction, the formation of Fe₃Si within 2 min also shows that iron oxide reduction is faster than silica [23], and a small amount of reduced silica dissolved into the molten iron to form iron silicide. However, over time as more silica is reduced to silicon, structural composition of iron silicide changes from Fe₃Si to Fe₅Si₃, which indicates that amount of silicon in iron silicide was increasing. Simultaneously, some carbon also dissolved into iron, and solute carbon is much more reactive than the solid carbon for silica reduction [23, 24]. The reduction of iron oxide produced CO gas which also helps in the gas-phase reduction of silica [20].

SEM image in Fig. 9 shows various phases as the reactions progressed over time, and these are comparable with XRD results. Three distinct phases were observed in the pellet images indicating changes associated with them at different reduction times that were analyzed by EDS spectra (Fig. 6). At lower magnification 55 ×, three images were taken at different reduction times (2, 4, and

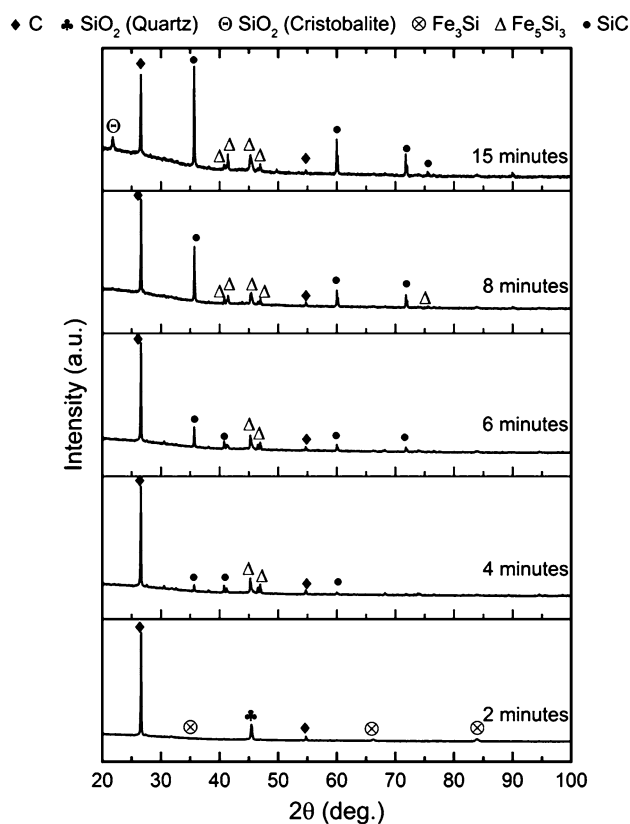


Fig. 8 X-ray diffraction spectra of the reduced pellet at different reduction times

15 min) in the hot zone. The darker part in the SEM images in Fig. 9 (2 and 4 min) represented carbon content due to the availability of excess carbon. However, some areas darker than carbon were observed, but these were the pores that can be attributed to gas-phase reactions. The presence of metallic phase with bright color was attributed to Fe₅Si₃-recovered phase with a small amount of carbon being dissolved as observed in the previous EDS analysis (Fig. 6). The gray phase showed high Si peak in Fig. 6 and was attributed to the formation of SiC. Comparing the images (Fig. 9) over a time period of 2–15 min, it was observed that the SiC-containing phases were increasing with the increasing time.

Infrared gas analyzer used in this work was able to detect CO, CO₂, and CH₄ gases, but not SiO gas. Nevertheless, it has already been proven that in silica reduction, reactions proceed via the intermediate silicon monoxide gas (SiO) [17, 23]. Figure 10 shows plot of gas evolution at the constant temperature of 1,550 °C during reduction. The volume concentrations (Parts per million, ppm) of CO, CO₂, and CH₄ off gases were converted into moles using standard gas equation. By analyzing the gas evolution, it can be seen that within 15 min, the reaction had become relatively slow as seen from the low levels of gas

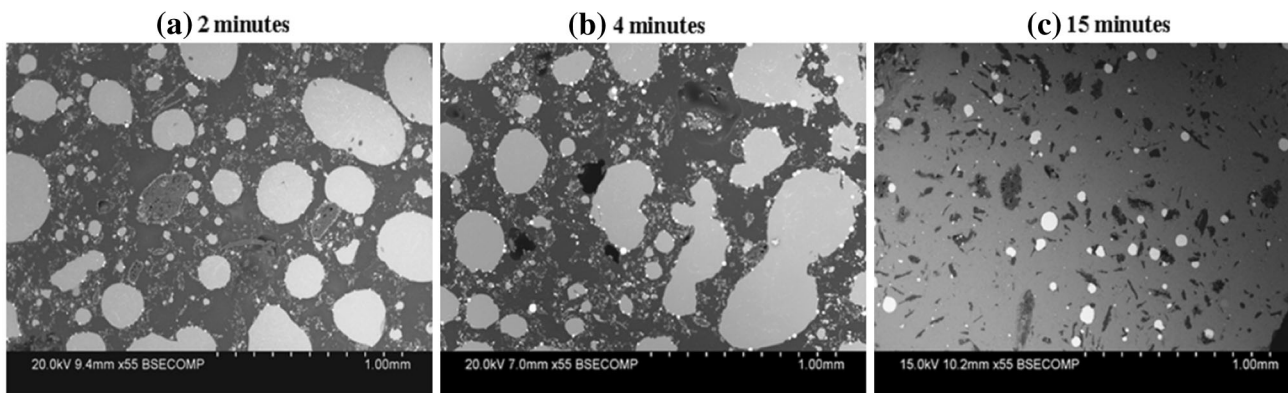


Fig. 9 SEM images to establish changes in phases at different reduction times

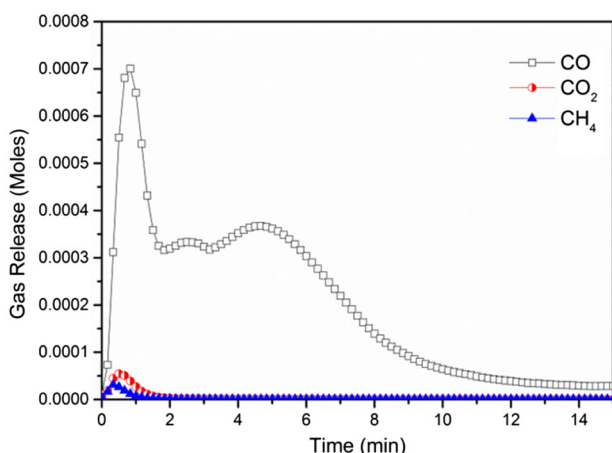


Fig. 10 Number of moles of CO, CO₂, and CH₄ gases released over time at temperature 1,550 °C

generated. Initial CO₂ release was negligible compared to CO generation, and almost zero for the rest of the reaction time. CH₄ release coming from Bakelite was also low, though the gas helped silica reduction and iron oxide reduction [11, 20]. In contrast, CO which is the evolved gas for silica as well as iron oxide reduction reactions showed three humps. The profile of CO release could be used as the basis to explain the reduction reactions along with XRD, SEM, and EDS data. As seen in Fig. 10, within 2 min, the sample showed the first sharp hump, and it was attributed to thermal degradation of Bakelite and catalytic effect of iron on Boudouard reaction [25] (reaction 4), and oxidation of C to CO has been known to have a strong influence on the reduction process [25]. Iron oxide reduction (reaction 1–3) was more dominant than the silica reduction (reaction 5–7) during this time period. It is generally considered that iron and silicon with different contents can result in different iron silicides such as Fe₃Si, Fe₂Si, Fe₅Si₃, FeSi, and FeSi₂, according to the Fe–Si binary phase diagram (Fig. 11) due to interdiffusion during solidification

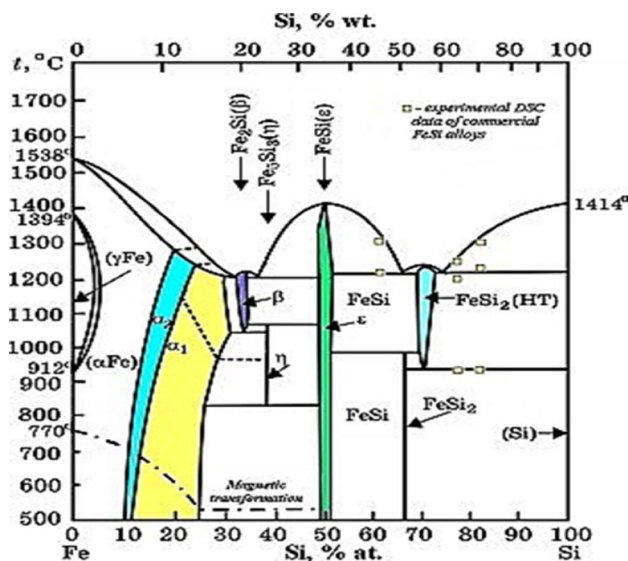
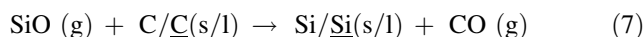
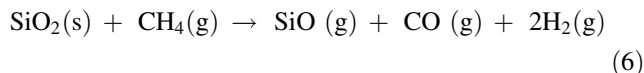
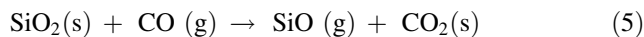
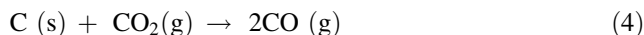
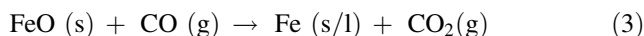
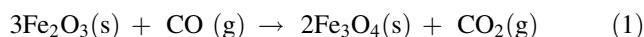


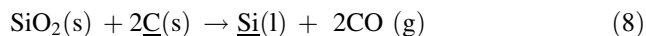
Fig. 11 Fe–Si Phase Diagram [26]

[26]. Therefore, during the rapid quenching from the hot zone (1,550 °C) to cold zone (~200 °C), a number of silicides formed depending on temperature and Si concentration. Fe₃Si was detected in XRD within 2 min, and after 4 min period, XRD detected Fe₅Si₃.

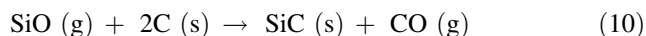
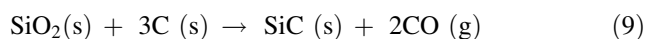


In the second small hump (Fig. 10), between 2 and 3.5 min, in the presence of molten iron, carbon dissolved

into iron, and solute carbon is available to participate in reduction reaction (reaction 7, 8) [23, 27]. Underlined elements represent the element in solution.



Finally, between 3.5 and 6 min, as shown in Fig. 10, moderate increase in CO was observed, and XRD detected high concentration of SiC over time. The reaction between silica in glass and carbonaceous material initiates at the contact point between SiO₂ and C. Once both SiO and CO are formed, the reactions proceed at the surfaces of both carbon and silica particles via gas phases. Some amount of SiO will be used in the system, and the remainder of the SiO will escape in the gas phase. Thus, some silicon loss could be attributed to the SiO gas escaping from the system prior to its conversion to SiC. Some reduced silica in the form of silicon, dissolved into the molten iron, while the rest of the silica reduced to SiC through solid (reaction 9)- and gas-phase (reaction 5, 10) reactions are expected. Besides, Boudouard reaction was also expected to contribute to the observed peak of CO gas. The formation of SiC retarded the reduction reaction by providing the physical barrier between reactants and caused a gradual decrease in CO gas evolution after 6 min.



The rate constant of silica reduction reaction was determined in terms of CO and CO₂ concentrations in the off gas mixture over time. The data on blank run (pellet containing graphite + bakelite + Fe₂O₃) gas release were deducted from the standard run (pellet containing graphite + bakelite + Fe₂O₃ + glass), so that only oxygen from silica in waste glass is taken into account for the calculation of silica reduction (assuming negligible effect of other

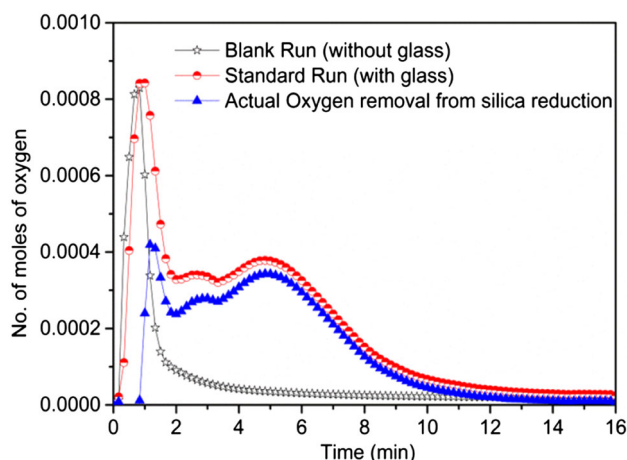


Fig. 12 Number of moles of oxygen removed over time

oxides in glass). Blank run was conducted under the same experimental condition. As a result, the rate of silica reduction reaction is obtained from the rate of oxygen removal from silica in glass. Figure 12 showed the oxygen release curves for standard run and blank run, and subtracted curve that gives the actual oxygen release only from silica in glass. Let, initially at time, $t = 0$, the number of moles of oxygen present in SiO₂ be W_0 , and at time t , W_t be the number of moles of oxygen remaining in the unreduced silica. So, the oxygen removal fraction or reduction extent (X) was calculated by Eq. 11:

$$\text{Reduction Extent } (X) \text{ in } \% = (W_0 - W_t)/W_0 \times 100 \quad (11)$$

W_t was measured by the following Eq. 12, where W_{CO} and W_{CO_2} are the moles of oxygen carried by CO and CO₂, respectively.

$$W_t = W_0 - (W_{\text{CO}} + W_{\text{CO}_2}) \quad (12)$$

Figure 13 shows the cumulative oxygen removal over time from silica in glass reduction reactions (The data point at time, $t = 1$ min of actual oxygen removal from silica reduction in Fig. 12, is considered as $t = 0$ data in Fig. 13). Reduction rate in terms of oxygen removal was almost linearly proportional over time up to 6 min although the reduction rate became slower afterward. The initial pellet containing glass comprised 0.0275 mol of oxygen in silica, and 0.0127 mol of oxygen was released due to reduction reactions of silica in glass in 15 min. Thus, reduction extent is around 46 % based on the calculation of moles of oxygen removed. Deposition of oxides such as Ca and Mg from glass and Bakelite as well as the formation of SiC slowed down further reduction.

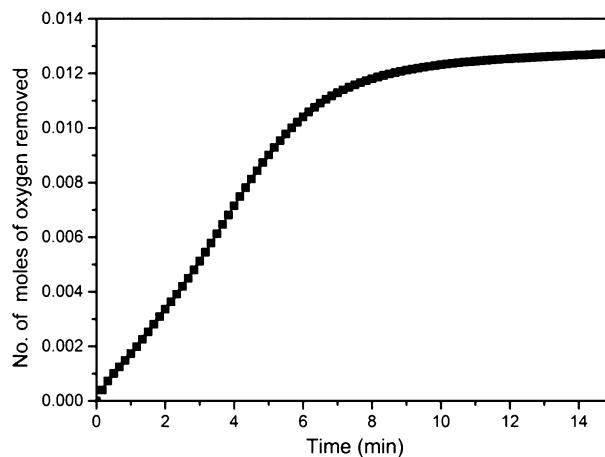


Fig. 13 Number of cumulative moles of oxygen removed as a function of time, during the reduction reaction of silica in waste glass at 1,550 °C

Assuming that the reduction process follows first-order reaction kinetics [28], the rate constant of the reaction was determined using the first-order reaction equation:

$$\text{Rate} = -\frac{d[W]}{dt} = k[W] \tag{13}$$

By integrating the equation (from $t = 0$ to t),

$$\ln[W_t] = -kt + \ln[W_0] \tag{14}$$

$$\ln \frac{W_t}{W_0} = -kt \tag{15}$$

$$\ln(1 - X) = -kt + c \tag{16}$$

Plotting $\ln(1 - X)$ against time, the rate constant k was determined by linear regression. Figure 14 shows the plot of $\ln(1 - X)$ against time (t). As two distinct slopes were observed, it can be concluded that different mechanisms were responsible for the reduction of silica in glass: the initial stage ($t \leq 400$ s) and latter stage ($t > 400$ s). The rate of silica reduction could be affected by various factors that influence either solid-state or the gas-phase reactions [28]. In previous analyses (XRD, SEM, and Gas data in Figs. 8, 9 and 10), it was shown that within 400 s, SiO formation and most of the SiC/Fe₅Si₃ formation occurred through the solid-state and gas-phase reactions. Afterward, SiC and other oxide deposition reduced the reaction rate which could explain the shift in mechanisms observed in the latter stage, showing a significant decrease in the rates of reduction reactions. In the initial stage ($t \leq 400$ s), the rate constant $k = 12.8 \times 10^{-4} \text{ s}^{-1}$ for the overall reduction of silica in glass is measured from the slope of the line within 0–400 s, shown in Fig. 15. The kinetics of silica reduction by graphite is controlled by both chemical reaction and mass transfer [28, 29]. Due to the deposition of the reaction product on graphite and silica, mass transfer is considered as the dominant mechanism at the end, and

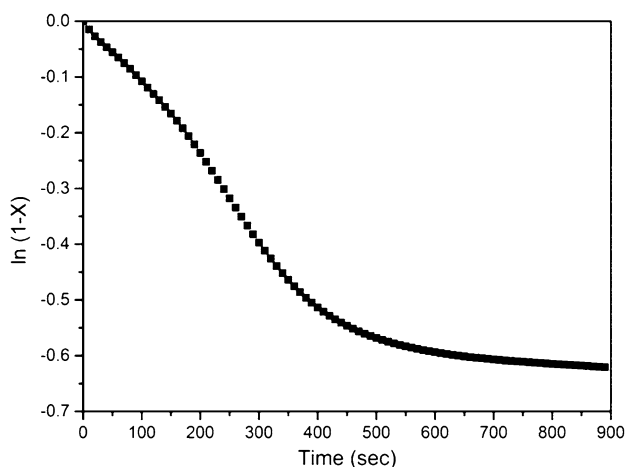


Fig. 14 Plot of $\ln(1 - X)$ as a function of time

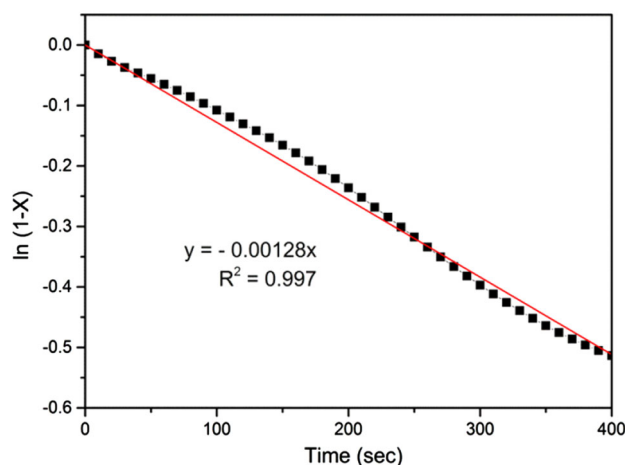


Fig. 15 Determination of reaction rate constant k , in the initial stage (time, $t \leq 400$ s) based on equation $\ln(1 - X) = -kt$

the chemical reaction is considered as the dominant mechanism at the start because of the high value of activation energy [28]. A similar behavior was also observed in the reaction kinetics of silica in waste glass. The rate of initial stage ($t \leq 400$ s) is considered to be predominantly controlled by chemical reactions dictating the reduction of silica in waste glass.

Conclusions

The major conclusions established by results are as follows:

- (1) The results of XRD, SEM, and EDS analyses confirmed the formation of SiC using waste automotive glass as silica source and blend of Bakelite and graphite as reducing agent. The reduced product of cubic β -SiC with other oxides (such as SiO₂, CaO, etc.) and excess carbon (graphite) can be used as a resource for composite refractory materials like SiC refractories, which may contain oxide/non-oxide or both. Addition of small amount of iron oxide increased the yield of SiC formation.
- (2) High-temperature observations coupled with XRD analysis and reduction studies showed that silica reduction reactions were dependent on time and SiC formation retards the reduction rate beyond a time period of about 6 min.
- (3) The rate constant for the initial stage ($t \leq 400$ s) was found to be $12.8 \times 10^{-4} \text{ s}^{-1}$ for silica reduction, and the overall reduction of silica was predominantly limited by the underlying chemical reactions governing the reduction.
- (4) This recycling approach creates a new input of raw materials resources for producing SiC-bearing

refractories such as furnace lining, insulating materials, etc. This approach also effectively provides a route to solve automotive waste glass and plastic disposal problem.

Acknowledgments The authors would like to acknowledge the financial support received from the Australian Research Council (ARC) and OneSteel for this project.

References

- Schei A, Tuset JK, Tveit H (1998) Production of high silicon alloys. Tapir, Forelag
- Liyang Z (2002) Energy optimization of the Acheson process for producing high purity silicon carbide. <http://www.ghi.rwth-aachen.de/www/pages/keramik/mitarbeiter/liyangzhou-aktuell-en.html>. Accessed 6 June 2014
- Erol MM, Kucukbayrak S, Ersoy-Mericboyu A (2006) The recycling of the coal fly ash in glass production. *J Environ Sci Health Part A* 41:1921–1929. doi:10.1080/10934520600779208
- Gazulla M, Gomez M, Orduna M, Barba A (2006) Physico-chemical characterisation of silicon carbide refractories. *J Eur Ceram Soc* 26:3451–3458. doi:10.1016/j.jeurceramsoc.2005.08.009
- Yang Y, Yang K, Lin Z-M, Li J-T (2007) Mechanical-activation-assisted combustion synthesis of SiC. *Mater Lett* 61:671–676. doi:10.1016/j.matlet.2006.05.032
- Anonymous (2002) Environmental impact of end-of-life vehicles: an information paper. Department of the Environment and Heritage 3:14
- S-I Sakai et al (2014) An international comparative study of end-of-life vehicle (ELV) recycling systems. *J Mater Cycles Waste Manag* 16:1–20. doi:10.1007/s10163-013-0173-2
- Szeteiová IK (2010) Automotive Materials Plastics in Automotive markets today. http://www.mtf.stuba.sk/docs/internetovy_casopis/2010/3/szeteiova.pdf. Accessed 3 Jan 2015
- Tupy M, Mokrejs P, Merinska D, Svoboda P, Zvonicek J (2014) Windshield recycling focused on effective separation of PVB sheet. *J Appl Polym Sci*. doi:10.1002/app.39879
- Sophia B (2011) Window glass recycling: difficult but not impossible. <http://1800recycling.com/2011/09/window-glass-recycling-difficult-not-impossible#sthash.MsdRSvHH.dpuf>. Accessed 6 June 2014
- Dankwah JR, Koshy P, Saha-Chaudhury NM, O’Kane P, Skidmore C, Knights D, Sahajwalla V (2011) Reduction of FeO in EAF steelmaking slag by metallurgical coke and waste plastics blends. *ISIJ Int* 51:498–507. doi:10.2355/isijinternational.51.498
- Sahajwalla V et al (2012) Recycling end-of-life polymers in an electric arc furnace steelmaking process: fundamentals of polymer reactions with slag and metal. *Energy Fuel* 26:58–66. doi:10.1021/Ef201175t
- Agarwal A, Pad U (1999) Influence of pellet composition and structure on carbothermic reduction of silica. *Metallurg Mater Trans B* 30:295–306. doi:10.1007/s11663-999-0059-9
- Biernacki J, Wotzak G (1989) Stoichiometry of the C + SiO₂ reaction. *J Am Ceram Soc* 72:122–129. doi:10.1111/j.1151-2916.1989.tb05964.x
- Chen S-H, Lin C-I (1997) Effect of contact area on synthesis of silicon carbide through carbothermal reduction of silicon dioxide. *J Mater Sci Lett* 16:702–704. doi:10.1023/A:1018508525803
- Koc R, Cattamanchi SV (1998) Synthesis of beta silicon carbide powders using carbon coated fumed silica. *J Mater Sci* 33:2537–2549. doi:10.1023/A:1004392900267
- Wiik K, Motzfeldt K (1996) Kinetics of reactions between silica and carbon and the formation of silicon carbide. *Mater Res Soc Symp P* 410:435–440. doi:10.1557/PROC-410-435
- Ju Z, Xu L, Pang Q, Xing Z, Ma X, Qian Y (2009) The synthesis of nanostructured SiC from waste plastics and silicon powder. *Nanotechnology* 20:355604. doi:10.1088/0957-4484/20/35/355604
- Meng S, Wang D-H, Jin G-Q, Wang Y-Y, Guo X-Y (2010) Preparation of SiC nanoparticles from plastic wastes. *Mater Lett* 64:2731–2734. doi:10.1016/j.matlet.2010.09.007
- Farzana R, Sahajwalla V (2013) Recycling automotive waste glass and plastic—an innovative approach. In *PRICM*, Wiley, Hoboken, pp 2267–2276. doi:10.1002/9781118792148.ch282
- Dhunna R, Khanna R, Mansuri I, Sahajwalla V (2014) Recycling waste bakelite as an alternative carbon resource for ironmaking applications. *ISIJ Int* 54:613–619. doi:10.2355/isijinternational.54.613
- Ozturk B, Fruehan RJ (1985) The rate of formation of SiO by the reaction of CO or H₂ with silica and silicate slags. *Metallurg Mater Trans B* 16:801–806. doi:10.1007/bf02667516
- McCarthy F, Sahajwalla V, Hart J, Saha-Chaudhury N (2003) Influence of ash on interfacial reactions between coke and liquid iron. *Metallurg Mater Trans B* 34:573–580. doi:10.1007/s11663-003-0026-9
- Khanna R, Ikram-Ul Haq M, Wang Y, Seetharaman S, Sahajwalla V (2011) Chemical interactions of alumina-carbon refractories with molten steel at 1823 K (1550 °C): implications for refractory degradation and steel quality. *Metallurg Mater Trans B* 42:677–684. doi:10.1007/s11663-011-9520-7
- Srinivasan N, Lahiri A (1977) Studies on the reduction of hematite by carbon. *Metallurg Mater Trans B* 8:175–178. doi:10.1007/bf02656367
- Gasik MM (2013) Handbook of ferroalloys: theory and technology. Butterworth-Heinemann, Oxford
- Ozturk B, Fruehan RJ (1985) Kinetics of the reaction of SiO(g) with carbon saturated iron. *Metallurg Mater Trans B* 16:121–127. doi:10.1007/bf02657497
- Sahajwalla V, Wu C, Khanna R, Saha Chaudhury N, Spink J (2003) Kinetic study of factors affecting in situ reduction of silica in carbon-silica mixtures for refractories. *ISIJ Int* 43:1309–1315. doi:10.2355/isijinternational.43.1309
- Sahajwalla V, Mehta AS, Khanna R (2003) Influence of chemical compositions of slag and graphite on the phenomena occurring in the graphite/slag interfacial region. *Metallurg Mater Trans B* 35B:75–83. doi:10.1007/s11663-004-0098-1